Accepted Manuscript

Simple one-step ultrasonic synthesis of anatase titania/polypyrrole nanocomposites

M.C. Arenas, L. Fernando Rodríguez, Domingo Rangel, O. Martínez-Álvarez, Claudia Martínez-Alonso, V.M. Castaño

PII: S1350-4177(12)00210-6
DOI: http://dx.doi.org/10.1016/j.ultsonch.2012.09.009
Reference: ULTSON 2194

To appear in: *Ultrasonics Sonochemistry*

Received Date: 23 July 2012
Revised Date: 6 August 2012
Accepted Date: 24 September 2012

Please cite this article as: M.C. Arenas, L. Fernando Rodríguez, D. Rangel, O. Martínez-Álvarez, C. Martínez-Alonso, V.M. Castaño, Simple one-step ultrasonic synthesis of anatase titania/polypyrrole nanocomposites, *Ultrasonics Sonochemistry* (2012), doi: http://dx.doi.org/10.1016/j.ultsonch.2012.09.009

This is a PDF file of an unedited manuscript that has been accepted for publication. As a service to our customers we are providing this early version of the manuscript. The manuscript will undergo copyediting, typesetting, and review of the resulting proof before it is published in its final form. Please note that during the production process errors may be discovered which could affect the content, and all legal disclaimers that apply to the journal pertain.

ACCEPTED MANUSCRIPT

Simple one-step ultrasonic synthesis of anatase titania/polypyrrole nanocomposites

M. C. Arenas[1]*, L. Fernando Rodríguez[1], Domingo Rangel[1], O. Martínez-Álvarez[2], Claudia Martínez-Alonso[3], V.M. Castaño[1]

[1]Departamento de Ingeniería Molecular de Materiales, Centro de Física Aplicada y Tecnología Avanzada, Universidad Nacional Autónoma de México, Boulevard Juriquilla 3001, Querétaro, Querétaro 76230, México.

[2]Ingeniería en Energía, Universidad Politécnica de Guanajuato, Av. Universidad Norte s/n, Juan Alonso Cortazar Guanajuato, C.P. 38438, México

[3]Centro de Investigación en Energía, UNAM, Priv. Xochicalco S/N, Temixco 62580, Morelos, Mexico

*Corresponding author: mcaa@fata.unam.mx

Phone: + 52- 44 22381173 ext. 132, +52 55 5623 4173 ext. 132

ACCEPTED MANUSCRIPT

Abstract

In this work, hybrid nanocomposites based on anatase titania:polypyrrole (TiO_2:PPy) were directly obtained from a simple, one-step, ultrasonic (UT)-assisted synthesis. The properties of these crystalline nanocomposites were compared with those of others fabricated using cold-assisted synthesis (Cold) without any UT assistance, which required a hydrothermal treatment (HT) to yield crystalline anatase titania in the nanocomposite (TiO_2:PPy) at low temperature (130 ºC) and in a short time (3 h). The SEM results demonstrated that the UT-assisted synthesis is a feasible method to obtain anatase TiO_2:PPy nanocomposites with controlled morphology using low energy. The Fourier transform infrared (FT-IR) bands of the crystalline nanocomposites exhibited a shift with respect to neat components, which was attributed to the strong interaction between the secondary amine groups (N-H) of PPy and the oxygen from TiO_2 . The acceptable absorption in the visible region (λ_{max}= 670 nm)

ACCEPTED MANUSCRIPT

indicates that these nanocomposites are good candidates for harvesting energy in solar cells. Devices based on these nanocomposites were built to evaluate their electrical properties. An increase in the photocurrent was observed for the devices prepared with the nanocomposites from the UT-assisted synthesis.

Keywords: *ultrasound, hybrid composites, polypyrrole, nanoparticles, titania*

1. Introduction

Titania (TiO_2) is an inorganic semiconductor with a large band gap (Eg), ranging from 3.2 eV to 3.7 eV [1], that is widely used mainly in photocatalysis [2, 3] and solar cells [4, 5] due to its excellent optical properties, effective electron transport and photoreaction activity. Anatase is the main crystalline phase used for these applications because it is a stable phase at room temperature and atmospheric pressure, unlike the boorkite or rutile phases [6, 7]. To transform amorphous TiO_2 into the anatase crystalline phase, certain treatments are required, for example, annealing at temperatures above 300 ºC [8-10], hydrothermal processing for up to 96 h [10-12], microwave-assisted hydrothermal methods with subsequent annealing at 450 ºC [13] or hydrothermal treatment at 200 ºC for 24 h [12, 13]. It is clear that a significant amount of energy and long times are required in these processes. In addition, to obtain ordered structures of anatase titania, hard template and/or an electrochemical deposition at a high applied potential are necessary [14, 15].To improve the optical absorption of anatase titania in the visible region, a doping process using several materials has also been implemented [16, 17]. For example, anatase TiO_2 has been doped with alumina (Al_2O_3) by combining two techniques (electrophoresis and sputtering), which reduced the large band gap of anatase TiO_2 to 2.87 eV;

ACCEPTED MANUSCRIPT

however, the TiO_2:Al_2O_3 ratio and the annealing temperature were critical parameters to achieve this reduction [16]. Doping with manganese, carbon or silver or co-doping with silicon-tungsten have recently been used to achieve the same goal; however, higher temperatures in the range of 400 ºC and 500 ºC are required [3, 17, 18]. Organic conducting polymers have been used in several devices (capacitors, light-emitting diodes, solar cells) because of their intrinsic conductivity induced by the redox doping process, flexibility and facile processability. Recently, conducting polymers such as polyaniline have functioned as dopants in shifting the border of the TiO_2 particles to longer wavelengths, thereby improving the optical absorption in the visible region that depends on the concentration of the conducting polymer [19]. These hybrid conducting polymer/TiO_2 composites present particular properties unlike those of the individual materials, such as controlled conductivity, thermal or mechanical stability, and these properties have made them potentially applicable as anode materials for lithium-ion batteries [20], anode electrodes for dye solar cells [19, 21] or photocatalytic materials [22, 23]. The preparation of these composites can involve an in-situ method, where the conducting polymer is synthesized in the presence of the defined particle size of the commercial anatase TiO_2 to form core-shell structures [19, 24]. These composites can also be prepared using a two-step electrochemical process, in which a TiO_2 nanotube film is anodized, and the conducting polymer is then electrodeposited onto the anodized nanotube film [22].

Herein, hybrid nanocomposites based on anatase TiO_2 and polypyrrole (PPy) using a simple, one-step, ultrasonic-assisted synthesis were prepared and compared with those fabricated using cold-assisted hydrothermal synthesis. The structural, morphological, intermolecular and thermal properties were studied using X-ray diffraction, SEM and HRTEM, FT-IR spectroscopy and TGA, respectively.

ACCEPTED MANUSCRIPT

2. Experimental section

2.1 Reagents

Nitric acid (HNO_3), ferric chloride (FeCl3), distilled pyrrole (Py) and titanium tetraisopropoxide ($Ti(OCH(CH_3)_2)_4$ were purchased from Sigma-Aldrich, and isopropanol (CH_3-CHOH-CH_3) was purchased from J.T Baker. Distilled water was also used.

2.2 Procedure

The procedure for synthesizing hybrid nanocomposites was based on reference [21] with several modifications. The synthesis was performed under ultrasound or cold conditions following the procedure described in Figure 1.

For the ultrasonic-assisted synthesis (UT), two solutions were prepared and rapidly mixed to begin the one-step synthesis of both components (polypyrrole and anatase titania). The first solution consisted of $FeCl_3$ as the oxidizing agent (2.350 g), distilled water (0.90 ml), HNO_3 (0.090 ml) and isopropanol (3 ml) stirred well using a magnetic stirrer in a beaker at room temperature. For the preparation of the second solution, the reagents were added in a beaker in the following order: isopropanol (2.4 ml), Py (0.98 ml) and $Ti(OPr)_4$ (4 ml), and the solution was promptly mixed with the first solution. Immediately, the mixture was covered and stored under ultrasound conditions (100 W, 42 kHz ±6%) for 1 h. The color of the mixture changed from transparent to dark blue, which is the characteristic color of PPy. After 1 h, the mixture was stored at rest for 12 h, and then the homogeneous crystalline product was washed several times with isopropanol to remove any remnants, which were dispersed in the same solvent.

ACCEPTED MANUSCRIPT

For the cold-assisted synthesis (Cold) without ultrasonic assistance, a similar procedure to the UT synthesis was implemented; however, the temperature of the first solution was maintained at approximately 5 ºC, while the second solution was being prepared. The mixture was stored at 1 h at 5 ºC - 7 ºC and remained at rest for 12 h, and then the dark amorphous product was washed with isopropanol and dispersed in the same solvent.

The fine, dark, crystalline nanocomposites from the UT and the amorphous composites from the cold-assisted synthesis were poured into a Teflon-lined autoclave for hydrothermal treatment at 130 ºC for 3 h or 24 h. Then, one portion of the composites was dried at 70 ºC for 24 h in a vacuum oven for the post-characterizations. The samples will be labeled as Cold and UT for the low temperature and ultrasound-assisted systems, respectively, and the hybrid composite that was hydrothermally treated will be labeled with HT.

2.3 Characterization

For the Fourier transform infrared (FT-IR) spectroscopy characterization, nanocomposite powder (approximately 1%) mixed with potassium bromide (KBr) was prepared to obtain nanocomposite KBr pellets. A Rigaku MiniFlex+ X-ray diffractometer using CuKα radiation was used to determine the crystallinity of the nanocomposite powder.

SEM morphology and EDS analysis were performed using a JEOL microscope model JSM- 6060 L. High-resolution transmission electron microscopy (HRTEM) was performed in a JEOL JEM-2010 at 200 KV. For SEM and HRTEM, the samples were dispersed in isopropanol and sonicated for

ACCEPTED MANUSCRIPT

approximately 20 min before placing them on SEM stubs or TEM Formvar carbon-coated grids. For UV-Vis spectroscopy, the nanocomposite solutions were diluted in an isopropanol solution, and their properties were measured in a Spectronic Genesys 2PC spectrophotometer. Thermogravimetric analysis (TGA) of the nanocomposite powder was conducted in a TA Q500 TGA analyzer up 900 ºC at a scan rate of 10 ºC/min under nitrogen gas (N_2).

3. Results and discussion

The SEM morphology of the hybrid composites is presented in Figure 2. The composites fabricated using the cold-assisted synthesis contain agglomerates composed of particles, 110 nm ±25 nm in size (Figure 2a). When the composite is hydrothermally treated (HT) at 130 ºC for 3 h, irregular clusters of particles, approximately 113 nm ± 26 nm in size, are observed (Figure 2c). However, the composite produced using UT contains clusters of irregular particles with an average size of 121 nm ±26 nm (Figure 2b), while well-defined regular particles with an average diameter of 175 nm ±42 nm are observed in the hydrothermally treated UT composite (Figure 2d). Thus, the morphology and grain particle size of the nanocomposites depend on the ultrasound assistance or the hydrothermal treatment.

Broad peaks are observed in the XRD pattern (Figure 3) of the hybrid composite fabricated using cold-assisted synthesis, indicating that the composite is fully amorphous. However, well-defined sharp peaks are observed in the spectra of the UT-assisted synthesis hybrid composites, where the peaks at 2θ= 25.28º, 37.8º, 48.04º, 55º and 62.75º match with those of the anatase titania card (JCPDS 21-1272) [6], confirming the crystallinity and TiO_2 phase. Both composites were hydrothermally treated (HT),

ACCEPTED MANUSCRIPT

and the crystallinity of the TiO_2 was improved, mainly in the amorphous Cold composite (see Figure 3b and 3d).

The mechanism for the formation of the anatase phase in an acidic medium at a fast heating rate consists of the following steps: the 6-fold coordinated structures ($[Ti(OH)_x(OH_2)_{6-x}]_{(4-x)}^{+}$) (amorphous aggregate) produced by the mixture of the alkoxide precursor with water condenses to produce octahedra (TiO_6^{2-}) that are free in solution. When the solution is promptly heated, the isolated octahedra act as seeds or nucleation centers, and the heating promotes the arrangement of the four edges shared per octahedron, the characteristic structure of the anatase phase of TiO2[7].
In this work, the pH of the solution was approximately 4, and the precipitation of anatase nanocrystals was directly obtained with ultrasonic assistance. This process is explained by the acoustic cavitation phenomena, where the implosive collapse of bubbles in a liquid, higher local temperatures (above 5000 K), higher pressures (>20 MPa) and higher cooling rates (1010 K/s) promote the formation of crystalline phase nuclei [25, 26]. The optimization of the anatase phase under hydrothermal conditions, however, has been explained to occur in two stages; in the first stage, solid-state epitaxial growth occurs (fast growth rate) and in the second stage, dissolution and deposition occur (slow growth rate) [27, 28].

The grain size of the TiO_2 was determined from the diffraction peak of the anatase in the (101) plane using Scherrer's equation [6]. The values calculated are presented in Table 1. It is clear that a short HT time (3 h) in a hybrid composite produced using cold-assisted synthesis is sufficient to transform the amorphous phase of titania to the anatase phase with an average grain size of 3.49 nm, which increases to 4.735 nm after 24 h of HT. The UT-assisted composite had a grain size of 3.59 nm without any HT, and the grain size increased to 5.07 nm after a 24-h hydrothermal treatment.

ACCEPTED MANUSCRIPT

These results indicate that a similar grain size of approximately 3.5 nm can be obtained from UT and cold-assisted synthesis; however, in the latter, a hydrothermal treatment of 3 h is required, while in the former, this treatment is not necessary. Thus, UT assistance is a feasible route to directly obtain crystalline anatase TiO_2 in a hybrid composite using lower energy and without any HT compared with other procedures, where high temperatures between 350 ºC to 550 ºC are necessary to obtain this phase [1, 2, 8]. In our case, these higher temperatures could affect the properties of the PPy. In addition, the grain size could be increased by 25% of its value with a short hydrothermal treatment.

The average grain size of the neat TiO_2 at 3 h of HT was 5.35 nm (Figure S1a of supplementary document.); therefore, the growth of TiO2 is not affected during the synthesis of the hybrid composites. PPy is fully amorphous according to the XRD results (Figure S2 of supplementary document).

The validation of the presence of PPy and TiO_2 in the amorphous and crystalline hybrid nanocomposites was performed using FT-IR spectroscopy in the range of 1800 to 550 cm^{-1} (Figure 4). The PPy and TiO_2 spectra are included, and their characteristic bands are marked for comparison with the nanocomposite spectra. Pure anatase TiO_2 exhibits peaks at 1624 cm^{-1} and 1380 cm^{-1} and a broad peak in the range of 1000 cm^{-1} to 500 cm^{-1}; the latter is attributed to the Ti-O-Ti bond of the crystalline phase [8]. Other peaks at 3450-3300 cm^{-1}, 1639-1630 cm^{-1} and 660-634 cm^{-1} have been reported for nanoporous TiO_2 fabricated using the plasma-enhanced chemical vapor deposition (PECVD) process [8] or for commercial nanoparticles [24]. Based on these results, all the crystalline hybrid composites exhibit the main peak (1000 cm^{-1} to 500 cm^{-1}) of neat anatase TiO_2; however, this peak is slightly shifted to a shorter wavenumber (800-500 cm^{-1}), which is in concordance with the literature [29-31], unlike the amorphous composite from the cold-assisted synthesis.

ACCEPTED MANUSCRIPT

Table 2 presents the IR bands of the pure PPy [30-33] compared with all the peaks of the hybrid nanocomposites. Almost all the peaks of the neat PPy are present in all the nanocomposites; however, they are shifted to larger wavenumbers, which could be due to the strong interaction between the nitrogen atom of PPy and the TiO_2 nanoparticles. Titanium is a transition metal, and titania tends to form coordination compounds with nitrogen atoms [31].

The thermal stability of the amorphous and nanocrystalline hybrid composites was examined using thermogravimetric analysis (Figure 5) at a heating rate of 10 ºC/min under N_2. The TGA profile of all the composites exhibits three stages of weight loss in the range of 60 ºC to 850 ºC. The first stage appears between 30 ºC to 100 ºC, which could occur because of the moisture and the remnant O-Ti-O hydroxyls in the composites. The second and third stages may result from the degradation of the composites, where the behavior of each profile depends of the Cold and UT conditions or the hydrothermal treatment, according to the derivate graphic (DTGA, not presented here). The composites that underwent HT treatment exhibit slow degradation in the range of 140 ºC to 600 ºC, while the degradation of those without HT occurs between 140 ºC and 500 ºC. This phenomenon could be attributed to the crystallinity of the TiO_2 or the strong electrostatic interactions of TiO_2 with the functional groups of PPy.

The temperature of the maximum rate of degradation (T_{max}) of the moisture (first stage) and the decomposition of the composites (second and third stages), the onset decomposition temperature (Temp. onset) after the moisture weight loss and the percentage of the weight loss acquired from the DTGA graphics are summarized in Table 3. In the first stage, the composites exhibited a weight loss

ACCEPTED MANUSCRIPT

due to moisture in the range of 8 - 12 %, and this value was reduced to 5 - 7 % in the composites hydrothermally treated for 3 h. In the second stage, both the crystalline composites that were hydrothermally treated exhibited a major weight loss (20 - 26 %), and they are 40 -50 ºC more stable than the composites without any hydrothermal treatment. Therefore, it is clear that the hydrothermal treatment improves the thermal stability of the composites.

The UV-Vis spectra of the crystalline hybrid composites with hydrothermal treatment (UT-HT and Cold-HT) are presented in Figure 6a. The neat TiO_2 and pure PPy spectra are presented as references. The neat anatase TiO_2 exhibits an absorption edge at 375 nm (the maximum absorption in the blue region), and the neat PPy absorbs above 500 nm (the visible and near IR regions). It is clear that the high absorption of the PPy in the IR region (beyond 760 nm) of the free carrier tail (delocalized conjugation length) is due to the extended coil chain [35].

In the Cold-HT hybrid nanocomposite, the absorption of both components in the blue zone due to the TiO_2 and in the visible region due to the PPy are observed. However, the absorption edge of the TiO_2:PPy composite is shifted 20 nm to longer wavelengths compared with the neat TiO_2. In the UT-HT composite, a well-defined band in the visible region is observed at 670 nm, which is attributed to the PPy absorption (see inset of Fig. 6a) and indicates that these composites could be useful in harvesting energy for optoelectronic applications, such as in photovoltaic devices. Similar shifts have been observed in biomorphic TiO_2 produced using ultrasonication and subsequent annealing at 450 ºC [36].

The direct optical transition of the composites was calculated using the equation: $\alpha h\nu = A(h\nu - Eg)^p$, where α is the absorption coefficient, $h\nu$ is the photon energy, Eg is the optical band gap, p is assumed to be 0.5 for the direct transition and A is a constant concerning the transition probability. The direct

ACCEPTED MANUSCRIPT

transition of PPy and TiO_2 was calculated based on reports [6], and then, this transition was used to determine the Eg of the hybrid composites. The $h\nu$ *vs.* $(\alpha h\nu)^2$ plots of the hybrid composite and the reference materials (PPy and TiO_2) are presented in Figure 6b.

The estimated Eg value of neat TiO_2 is approximately 3.64 eV, which is in agreement with the values reported in the literature (which range from 3.2 to 3.8 eV) [1]. The Eg value reported for neat TiO_2 is 3.38 eV using the sols method [6], and it can be modified from 3.09 to 3.54 eV depending on the preparation conditions [37], where a wide optical band gap is related to the lack of impurities and defects [1]. The Eg of the hybrid composites is 3.25 eV for Cold composites and 3.4 eV for the UT composites. These values are slightly lower than the Eg of TiO_2, indicating that PPy is sensitized to the TiO_2.

The HRTEM images (Figure 7) illustrate the morphology of the hybrid composites fabricated using cold- and UT-assisted synthesis with HT at 3 h. Both hybrid composites contain agglomerates composed of amorphous PPy and crystalline TiO_2, in which nanocrystals are embedded in the amorphous PPy. Statistical distributions (not presented here) indicated that the average of the grain diameters were 4.65 nm ±1.65 nm and 4.81 nm ±0.89 nm for the Cold and UT hybrid composites, respectively. The lattice spacing of approximately 3.7 Å observed in the images corresponds to the (101) planes of anatase TiO_2 [6], which indicates that the hybrid nanocomposites are composed of nanocrystalline TiO_2.

According to the TEM results, the neat TiO_2 had an average grain size of 4.72 nm ±0.89 nm (Figure S1b of the supplementary document), which means that the grain size values from the HRTEM results are slightly higher (~1 nm) than those values obtained from the X-ray diffraction patterns. However, the values are in the range of the deviation of the average grain size obtained using HRTEM.

ACCEPTED MANUSCRIPT

The atomic percentages from the EDS patterns (not presented here) of the hybrid composite are listed in Table 4. Carbon and oxygen are the main elements in the Cold and UT composites, which agree with the chemical composition of polypyrrole and TiO_2. Assuming that the monomer and TiO_2 precursor are fully consumed during the synthesis, the estimated molar ratio is approximately 6.5:2.5 in the TiO_2:PPy composites. The remnant of approximately 1% could be due to the carbon and oxygen from the moisture in the nanocomposites (isopropanol or water), and the presence of Fe and Cl elements could result from residual oxidizing agent ($FeCl_3$).

One-step ultrasound-assisted synthesis is a practical and simple method to obtain anatase-TiO_2:PPy nanocomposites in regular particle form, where the direct formation of the crystalline anatase TiO_2 observed in X-ray patterns is attributed to the cavitation phenomena. However, in the cold-assisted synthesis, hydrothermal treatment is necessary to obtain crystallinity in the composites, but at low temperatures and for short times. Both hybrid composites are good absorbing materials in the visible spectrum, and they could be potential candidates for harvesting visible light for solar cells. Anatase TiO_2 is an inorganic, n-type semiconductor and PPy is a p-type, organic semiconductor forming an acceptor/donor junction (hybrid heterojunction). According to the flat energy band diagram (Figure 8), the electronic transport of carrier charge could occur easily from TiO_2 to PPy. Jeong and coworkers [21] observed photoelectric conversion of approximately 0.015% in this type of structure ITO/TiO_2:PPy/Al by modifying the PPy concentration. In addition, recently, a photovoltaic response was observed in a commercial titania:polyaniline composite sandwiched between two ITO substrates [19].

Similar structures were fabricated with the hybrid composites (ITO/TiO_2:PPy/ITO) synthesized in this work to evaluate their electrical properties (current *vs.* potential curves) in the dark and under illumination (68820 Oriel Solar simulator, Universal Power Supply, 400-1000w). Figure 9 presents the linear and logarithmic I-V curves of devices composed of UT and Cold nanocomposites. The Cold

ACCEPTED MANUSCRIPT

composite exhibits a similar current *vs.* voltage response under the dark or illuminated conditions, while the UT composite exhibits current intensity results almost one order of magnitude greater than those of the Cold composite in the dark condition. Furthermore, an appreciable magnification of the current is observed when the UT device is illuminated (inset of Figure 9). Hence, the difference in their electrical properties could be due to the assistance of ultrasound leading to the creation of a UT composite with more regular morphology and better homogeneity and dispersibility in solution in comparison with the Cold composites.

The absence of the photovoltaic effect could be due to either the high TiO_2:PPy ratio (6.5:2.5) or the remnant of reagents in the composites. Michael [19] observed that the ideal concentration of the conducting polymer is approximately 10% in commercial titania:polyaniline to obtain a photovoltaic response. However, Jeong observed that the photoelectric efficiency conversion increased at a high concentration of polymer [21]. Therefore, a systematic study of these specific hybrid nanocomposites as a function of the PPy concentration is necessary and will be considered in future works.

4. Conclusion

Crystalline hybrid composites (TiO_2:PPy) were successfully obtained directly from a simple, one-step, ultrasonic-assisted synthesis using lower energy and without any HT compared with the amorphous composites obtained from cold-assisted synthesis, in which the crystalline anatase TiO_2 must be induced by a hydrothermal treatment. According to the optical results and energy band diagram, both the Cold and UT composites are good candidates for harvesting energy for optoelectronic devices, such as solar cells. However, a photocurrent was observed only in the devices with the UT

ACCEPTED MANUSCRIPT

nanocomposites, suggesting a systematic study to determine the optimal concentration of PPy, which will be considered in future work to improve the photoelectric response.

Acknowledgments

This work was financed by DGAPA-UNAM through Project PAPIIT-DGAPA (IB101512) and CONACyT-México (CB176450). The authors are grateful for the technical support received from Beatriz Millán, Genoveva Hernández, Alicia del Real, Lourdes Palma (INB-UNAM), Marina Vega (Geo-UNAM) and Patricia Altuzar (CIE-UNAM).

References

[1] Z. Wang, U. Helmersson, P.-O. Kall, Optical properties of anatase TiO_2 thin films prepared by aqueous sol–gel process at low temperature, Thin Solid Films 405 (2002) 50–54.

[2] P. Pulisová, J. Bohácek, J. Subrt, L. Szatmáry, P. Bezdicka, N. Murafa, anatase nanoparticles from hydrated titania gels, Catal. Today 161 (2011) 84–90.

[3] Q. Chen, H. Shi, W. Shi, Y.o Xu, D. Wu, Enhanced visible photocatalytic activity of titania–silica photocatalysts: effect of carbon and silver doping, Catal. Sci. Technol. 2 (2012) 1213-1220.

[4] S. V. Saji, M. Pyo, Dye sensitized solar cell of TiO_2 nanoparticle/nanorod composites prepared via low-temperature synthesis in oleic acid, Thin Solid Films 518 (2010) 6542–6546.

[5] C.-S. Chou, Y.-J. Lin, R.-Y. Yang, K.-H. Liu, Preparation of TiO_2/NiO composite particles and their applications in dye-sensitized solar cells, Adv. Powder Technol. 22 (2011) 31–42.

[6] Y. Sheng, L. Liang, Y. Xu, D. Wu, Y. Sun, Low-temperature deposition of the high-performance

ACCEPTED MANUSCRIPT

anatase-titania optical films via a modified sol–gel route, Opt. Mater. 30 (2008) 1310–1315.

[7] M. Gopal, W.J. Moberly Chan, L.C. De Jonghe, Room temperature synthesis of crystalline metal oxides, J. Mater. Sci. 32 (1997) 6001-6008.

[8] B. Korbely, Z. Nemeth, B. Reti, J. W. Seo, A. Magrez, L. Forro, K. Hernadi, Fabrication of homogeneous titania/MWNT composite materials, Mater. Res. Bull. 46 (2011) 1991–1996.

[9] N. Jagtap, M. Bhagwat, P. Awati, V. Ramaswamy. Characterization of nanocrystalline anatase titania: an in situ HTXRD study, Thermochim. Acta 427 (2005) 37-41.

[10] J.-M. Wu, X.-M. Song, M. Yan, Alkaline hydrothermal synthesis of homogeneous titania microspheres with urchin-like nanoarchitectures for dye effluent treatments, J. Hazard. Mater. 194 (2011) 338-344.

[11] T. Ban, Y. Tanaka, Y. Ohya, Fabrication of titania films by sol-gel method using transparent colloidal aqueous solutions of anatase nanocrystals, Thin Solid Films 519 (2011) 3468-3474.

[12] M. Ueda, Y. Uchibayashi, S. Otsuka-Yao-Matsuo, T. Okura, Hydrothermal synthesis of anatase-type TiO_2 films on Ti and Ti-Nb substrates, J. Allow. Compd. 459 (2008) 369-376.

[13] Peilin Zhang, Bin Liu, Shu Yin, Yuhua Wang, Valery Petrykin, Masato Kakihana, Tsugio Sato, Rapid synthesis of nitrogen doped titania with mixed crystal lattice via microwave-assisted hydrothermal method, Mater. Chem. Phys. 116 (2009) 269–272.

[14] L. Gang, L. Zhongqing, Z. Zhao, Y. Xin, Preparation of Titania Nanotube Arrays by the Hydrothermal Method, Chin. J. Catal. 30 (2009) 37–42.

[15] Shu-Yuan Wu, Wen-Chi Lo, Keh-Chang, Ju-Liang He, Study on the preparation of nao-flaky anatase titania layer and their photovoltaic application**,** Curr. Appl. Phys. 10 (2010) S180-S183.

[16] E. Barajas-Ledesma, M.L. García-Benjume, I. Espitia-Cabrera, M. Ortiz-Gutiérrez, F.J. Espinoza-Beltrán, J. Mostaghimi, M.E. Contreras-García, Determination of the band gap of TiO_2 –Al_2O_3 films as a function of processing parameters, Mater. Sci. Eng. B 174 (2010) 71–73.

ACCEPTED MANUSCRIPT

[17] C.Y.W. Lin, A. Nakaruk, C.C. Sorrell, Mn-doped titania thin films prepared by spin coating, Prog. Org. Coat. 74 (2012) 645–647.

[18] M. Sun, X. Cui, Anodically grown Si–W codoped TiO_2 nanotubes and its enhanced visible light photoelectrochemical response, Electrochem. Commun. 20 (2012) 133–136.

[19] M. Ibrahim, M. Bassil, U. B. Demirci, T. Khoury, G. El Haj Moussa, M. El Tahchi, P. Miele, Polyaniline–titania solid electrolyte for new generation photovoltaic single-layer devices, Mater. Chem. Phys. 133 (2012) 1040–1049.

[20] C. Lai, G.R. Li, Y.Y. Dou, X.P. Gao, Mesoporous polyaniline or polypyrrole/anatase TiO_2 nanocomposite as anode materials for lithium-ion batteries, Electrochim. Acta 55 (2010) 4567–4572.

[21] J.-D. Kwon, P.-H. Kim, J.-H. Keum, J. S. Kim, Polypyrrole/Titania hybrids: synthetic variation and test for the photovoltaic materials, Sol. Energy Mater. Sol. Cells 83 (2004) 311-321.

[22] H.-C. Liang, X.-Z. Li, Visible-induced photocatalytic reactivity of polymer–sensitized titania nanotube films, Appl. Catal. B: Environ. 86 (2009) 8–17.

[23] C. A. Coutinho, V. K. Gupta, Photocatalytic degradation of methyl orange using polymer–titania microcomposites, J. Colloid Interface Sci. 333 (2009) 457–464.

[24] X. Li, G. Wang, X. Li, D. Lu, Surface properties of polyaniline/nano-TiO_2 composites, Appl. Surf. Sci. 229 (2004) 395–401.

[25] P. E. Meskin, F. Y. Sharikov, V. K. Ivanov, B. R. Churagulov, Y. D. Tretyakov, Rapid formation of nanocrystalline HfO_2 powders from amorphous hafnium hydroxide under ultrasonically assisted hydrothermal treatment, Mater. Chem. Phys. 104 (2007) 439–443.

[26] J. Guo, S. Zhu, Z. Chen, Y. Li, Z. Yu, Q. Liu, J. Li, C. Feng, D. Zhang, Sonochemical synthesis of TiO_2 nanoparticles on graphene for use as photocatalyst, Ultrason. Sonochem. 18 (2011) 1082–1090.

[27] K. Yanagisawa, Y. Yamamoto, Q. Feng, N. Yamasaki, Formation mechanism of fine anatase crystals from amorphous titania under hydrothermal conditions, J. Mater. Res. 13 (1998) 825-829.

ACCEPTED MANUSCRIPT

[28] A. Matthews, The crystallization of anatase and rutile from amorphous titanium dioxide under hydrothermal condition, Am. Mineral. 61 (1976) 419-424.

[29] K.M.K. Srivatsa, D. Chhikara, M. S. Kumar, Synthesis of anatase Titania Nanostructures at Room Temperature by PECVD Technique, J. Mater. Sci. Technol. 27 (2011) 696-700.

[30] Z. Li, B. Hou, Y. Xu, D. Wu, Y. Sun, W. Hu, F. Deng, Comparative study of sol–gel-hydrothermal and sol–gel synthesis of titania-silica composite nanoparticles, J. Solid State Chem. 178 (2005) 1395–1405.

[31] C. Zhang, Q. Li, J. Li, Synthesis and characterization of polypyrrole/TiO_2 composite by in situ polymerization method, Synth. Met. 160 (2010) 1699–1703.

[32] Y. Jia, P. Xiao, H. He, J. Yao, F. Liu, Z. Wang, Y. Li, Photoelectrochemical properties of polypyrrole/TiO_2 nanotube arrays nanocomposite under visible light, Appl. Surf. Sci. 258 (2012) 6627–6631.

[33] J. Wu, Q. Li, L. Fan, Z. Lan, P. Li, J. Lin, S. Hao, High-performance polypyrrole nanoparticles counter electrode for dye-sensitized solar cells, J. Power Sources 181 (2008) 172–176

[34] P. Dallas, D. Niarchos, D. Vrbanic, N. Boukos, S. Pejovnik, C. Trapalis, D. Petridis, Polym. 48 (2007) 2007-2013.

[35] D. Zhang, X. Zhang, Y. Chen, P. Yu, C. Wang, Y. Ma, Enhanced capacitance and rate capability of graphene/polypyrrole composite as electrode material for supercapacitors, J. Power Sources 196 (2011) 5990–5996.

[36] J. Foroughi, G. M. Spinks, G. G. Wallace, Effect of synthesis conditions on the properties of wet spun polypyrrole fibres, Synth. Met. 159 (2009) 1837–1843.

[37] X. Liu, S. Zhu, H. Jiang, G. Zhou, Z. Chen, D. Zhang, Sonochemical replication of chloroplast with titania for light harvesting, Ultrason. Sonochem. 18 (2011) 1043-1047.

ACCEPTED MANUSCRIPT

Figure Captions

Figure 1. Flowchart of the experimental procedure of the cold- and UT-assisted synthesis.

Figure 2. SEM morphology of the hybrid composites prepared from a) cold- and b) ultrasound-assisted synthesis. c) and d) correspond to cold- and ultrasound-assisted composites undergoing HT at 130 ºC for 3 h.

Figure 3. X-ray patterns of hybrid composites prepared using cold- and ultrasound-assisted synthesis with and without HT at 130 ºC for 3 h.

Figure 4. FT-IR spectra of amorphous and crystalline hybrid nanocomposites from cold and UT-assisted synthesis. The spectra of neat PPy and TiO_2 are included for comparison.

Figure 5. TGA profiles of the amorphous and crystalline hybrid composites with and without hydrothermal treatment (130 ºC, 3 h).

Figure 6. a) UV-Vis spectra and b) $h\nu$ *vs.* $(\alpha h\nu)^2$ curves of the hybrid composites hydrothermally treated and dispersed in a solution of 2-propanol. The absorbance spectra of PPy and TiO_2 are included as references.

Figure 7. HTEM images of the hybrid composites synthesized under a) Cold and b) UT conditions and hydrothermally treated at 130 ºC for 3 h.

Figure 8. Energy band diagram of the hybrid composite, illustrating the carrier charge transport from the electron donor (PPy) to the acceptor donor TiO_2.

Figure 9. I-V curves in the dark (close symbols) and under illumination (open symbols) for the ITO/TiO_2:PPy/ITO devices prepared from the UT and Cold hybrid composites.

ACCEPTED MANUSCRIPT

Table captions

Table 1. Grain size of the titania in the hybrid composites estimated from XRD patterns using Scherrer's equation.

Table 2. Wavenumber and assignment of IR bands of PPy compared with the hybrid nanocomposites.

Table 3. Maximum and onset temperatures at different stages. The percentage of weight loss is included in brackets.

Table 4. Atomic percentage composition of the hybrid nanocomposites.

ACCEPTED MANUSCRIPT

ACCEPTED MANUSCRIPT

Supplementary Figures

Figure S1. a) X-ray diffraction patterns and b) TEM image of the neat titania obtained using UT-assisted synthesis at 130 ºC for 3 h.

Figure S2. X-ray diffraction pattern of the neat polypyrrole obtained using UT-assisted synthesis at 130 ºC for 3 h.

ACCEPTED MANUSCRIPT

ACCEPTED MANUSCRIPT

Table 1. Grain size of the titania in the hybrid composites estimated from XRD patterns using Scherrer's equation.

Composite	**Hydrothermal treatment time**	**Average grain size from XRD (nm)**
Cold	0	*Amorphous*
	3	**3.49**
	24	4.735
UT	0	**3.59**
	3	4.17
	24	5.07

ACCEPTED MANUSCRIPT

ACCEPTED MANUSCRIPT

Table 2. Wavenumber and assignment of IR bands of the neat PPy compared with the hybrid nanocomposites.

Wavenumber (cm^{-1}) and assignment of IR bands [30-34].	**Wavenumber (cm^{-1})**				
	neat PPy	**Amorphous**	**Cold w/HT**	**UT**	**UT w/HT**

ACCEPTED MANUSCRIPT

ACCEPTED MANUSCRIPT

	1714	1714	1683	1685	1685
1636.3, N-H in plane bending		1614	1606		
1560, C=C antisymmetric stretching	1581	1585	1581	1556	1560
1544, 1541.6, 1529 C=C antisymmetric stretching	1539	1529	1527		
1470, 1455.6, 1446 C=C symmetric stretching	1485			1485	1485
		1406	1400	1402	1400
			1325	1328	1330
1300, 1296.1, 1284 C-N and N-H deforming vibration	1284		1276	1288	1288
		1259			
	1222		1207	1201	1201
1175, C-N stretching					
1164.2, C-C stretching vibration					
1144, 1134, N=Q=N (Q is referred to pyrrole type rings)					
1042, C-C stretching vibrations		1051	1047	1049	1051
1030, 1034.5, C-H deformation vibrations and out-of-plane bending	1022			1004	1002
964, 963.7, doping state of PPy		945	950		
	939				933
916, 893.9, 887, doping state of PPy				929	
790, C-H deforming and wagging vibration		808			

ACCEPTED MANUSCRIPT

786.8, C-C stretching vibration	786		781	786	781
			734		736
	707	707			
680, 667.8, C- H out-of-plane bending					
	630	624	636	642	640

ACCEPT

ACCEPTED MANUSCRIPT

Table 3. Maximum and onset temperatures for different stages. The percentage of weight loss is included in brackets.

hybrid Composites	*Temp. max* (ºC) 1st step (moisture weight loss)	Temp. onset (ºC) after the moisture weight loss	*Temp. max* (ºC)	
			2nd step	3rd step
Cold TiO_2:PPy	65 (12%)	140	390 (16%)	773 (16%)
Cold TiO_2:PPy w/HT*	48 (5%)	144	**447 (20%)**	813 (14%)
TiO_2:PPy (UT)	40 (8%)	130	250 (18%)	772 (16%)
TiO_2:PPy (UT) w/HT*	43 (7%)	141	**283 (26%)**	475 (5%)

*Composites with better thermal stability

ACCEPTED MANUSCRIPT

ACCEPTED MANUSCRIPT

Table 4. Atomic percentage composition of the hybrid nanocomposites.

Composites from	**C %**	**N %**	**O %**	**Ti %**	**Fe %**	**Cl %**
Cold w/HT	54	2.4	30	9	0.6	4
UT w/HT	43	5	35	13	0.5	3.5

ACCEPTED MANUSCRIPT

Figure 1

ACCEPTED MANUSCRIPT

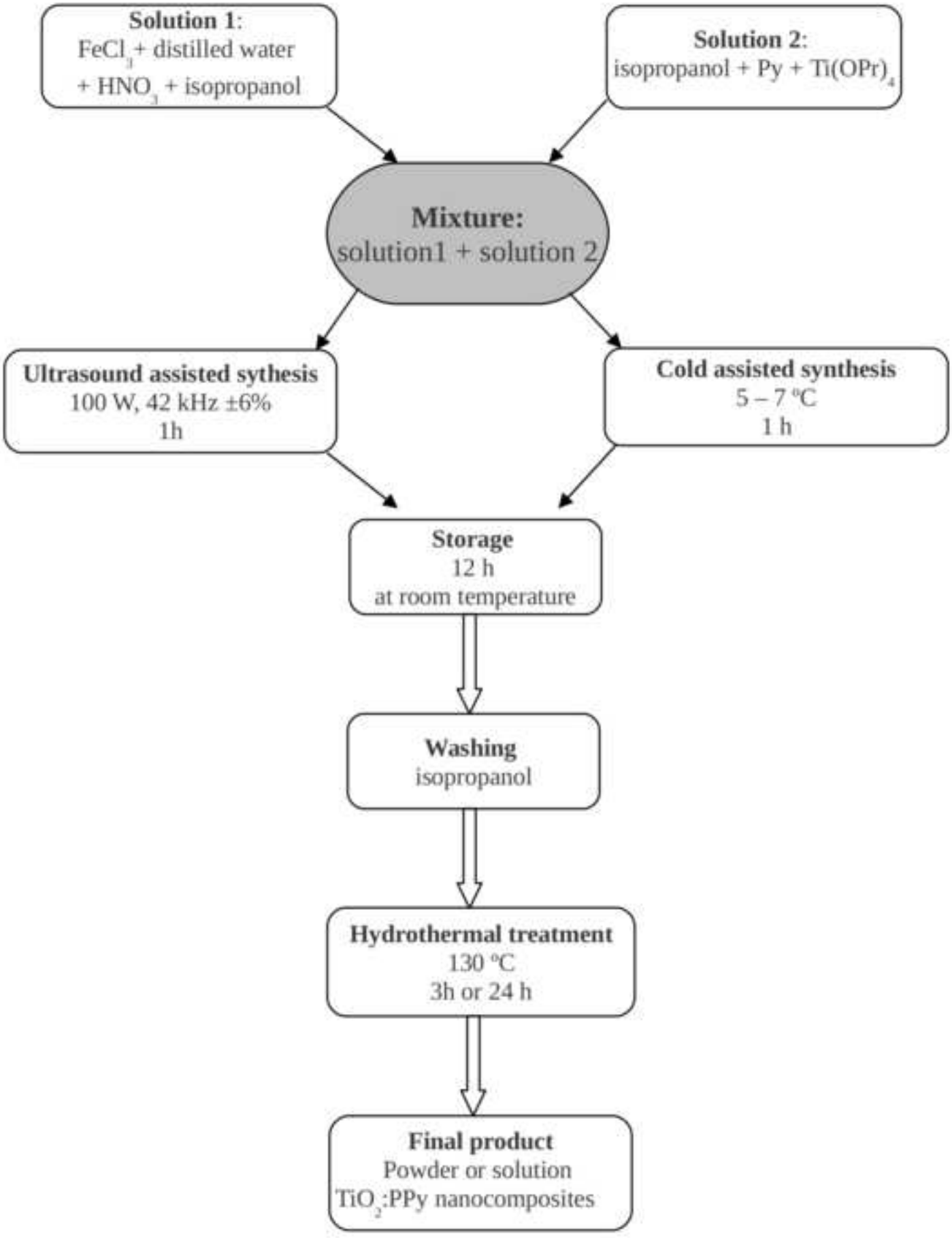

Figure 2

ACCEPTED MANUSCRIPT

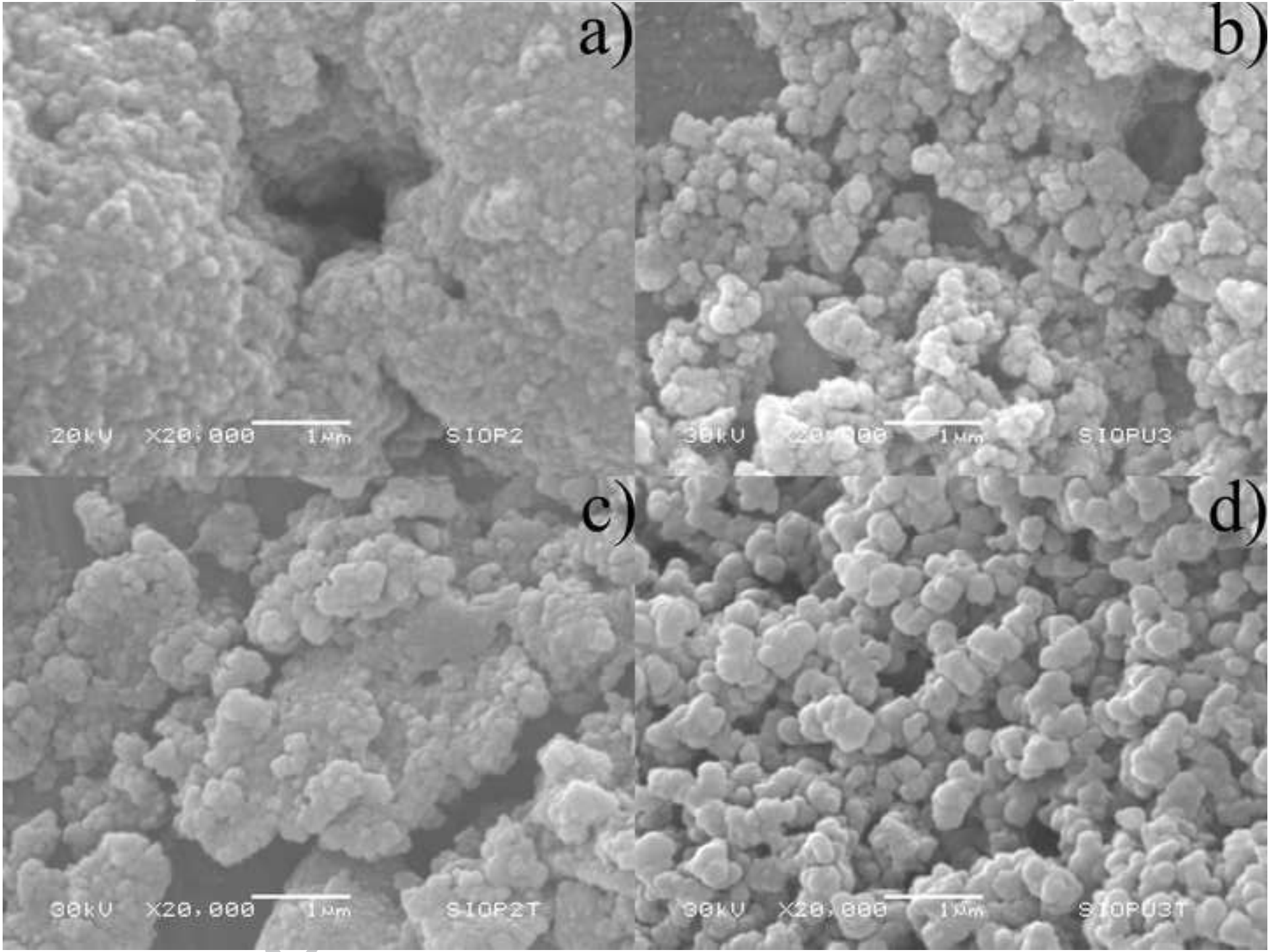

Figure 3

ACCEPTED MANUSCRIPT

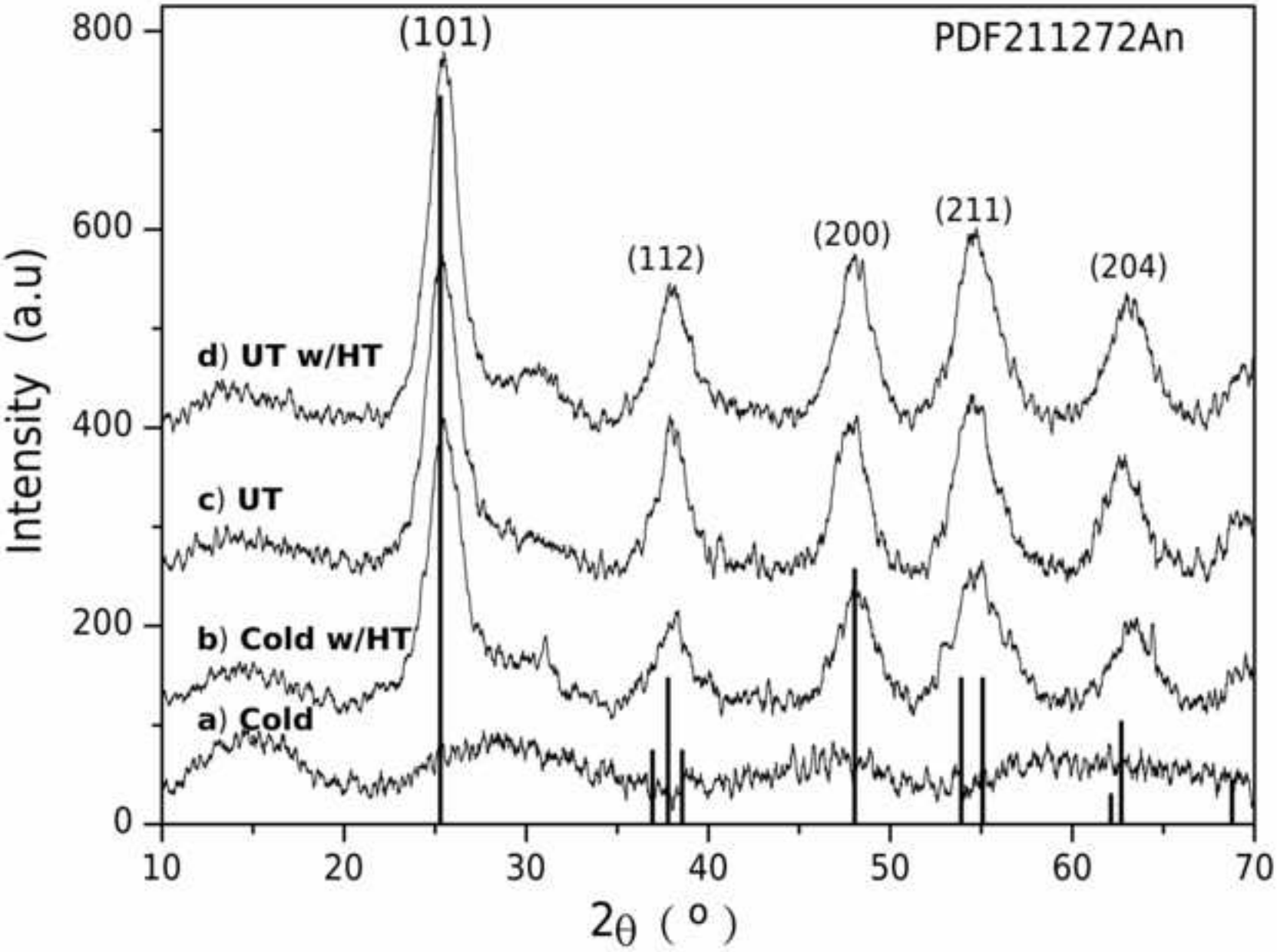

Figure 4

ACCEPTED MANUSCRIPT

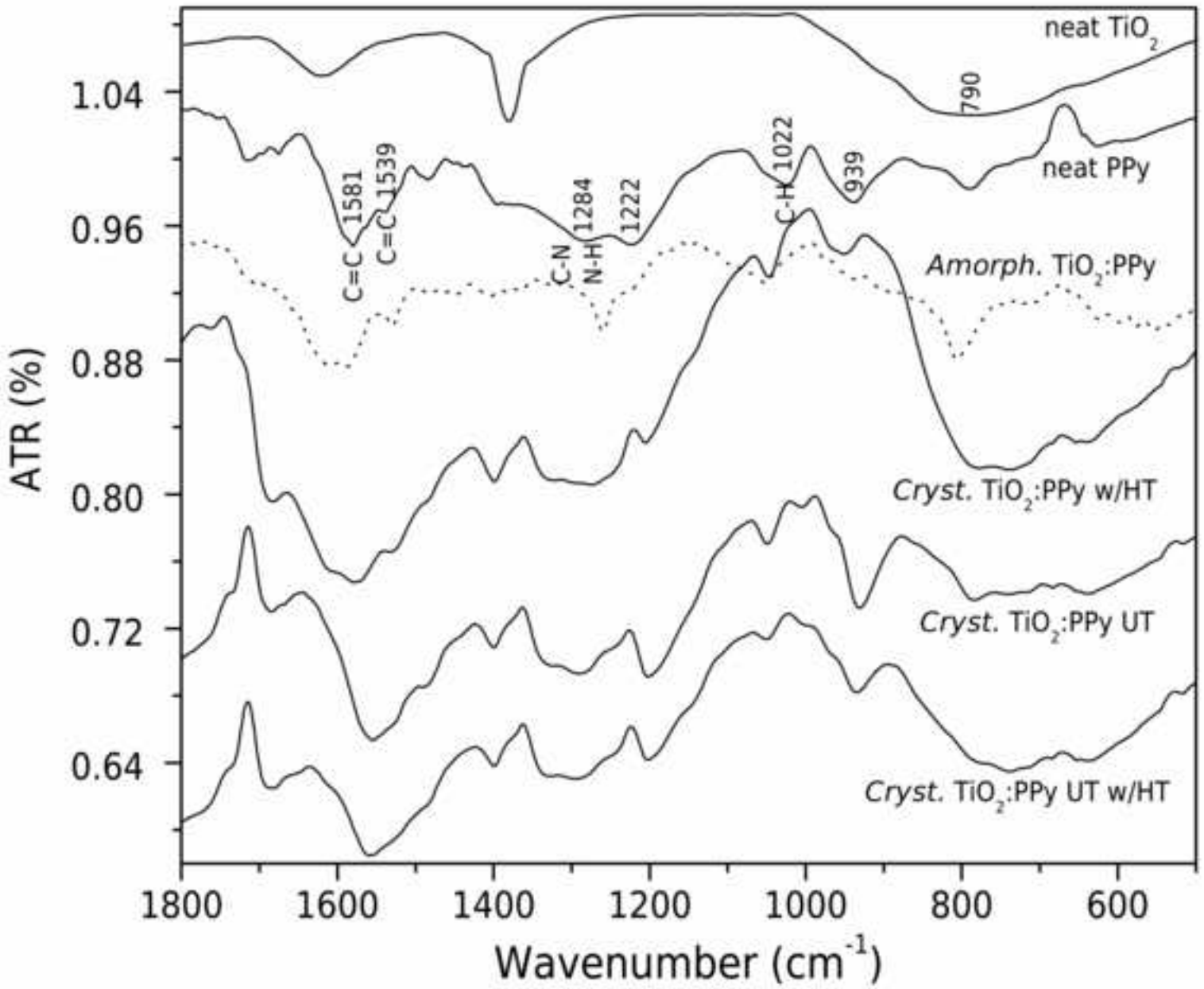

Figure 5

ACCEPTED MANUSCRIPT

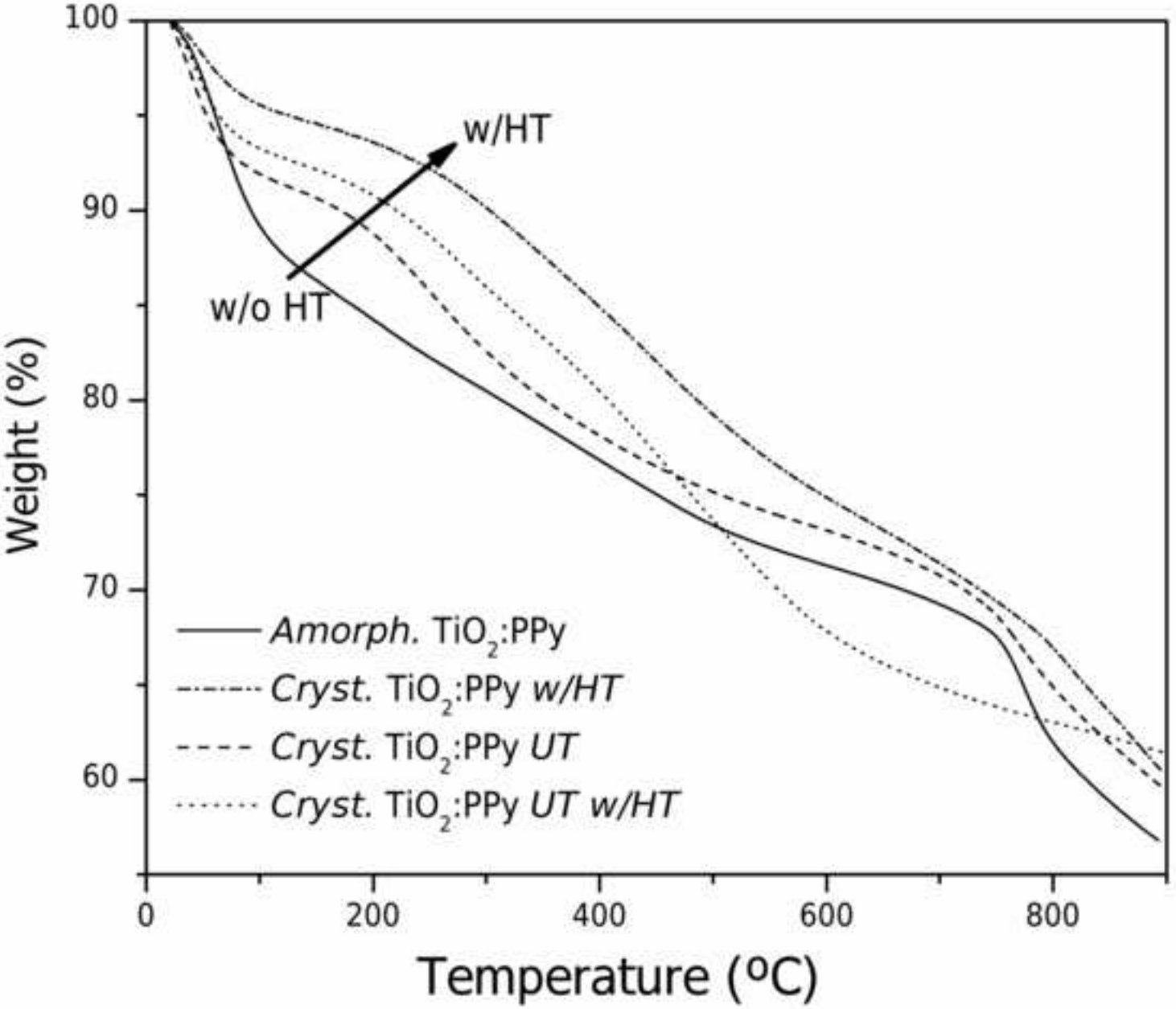

Figure 6a

ACCEPTED MANUSCRIPT

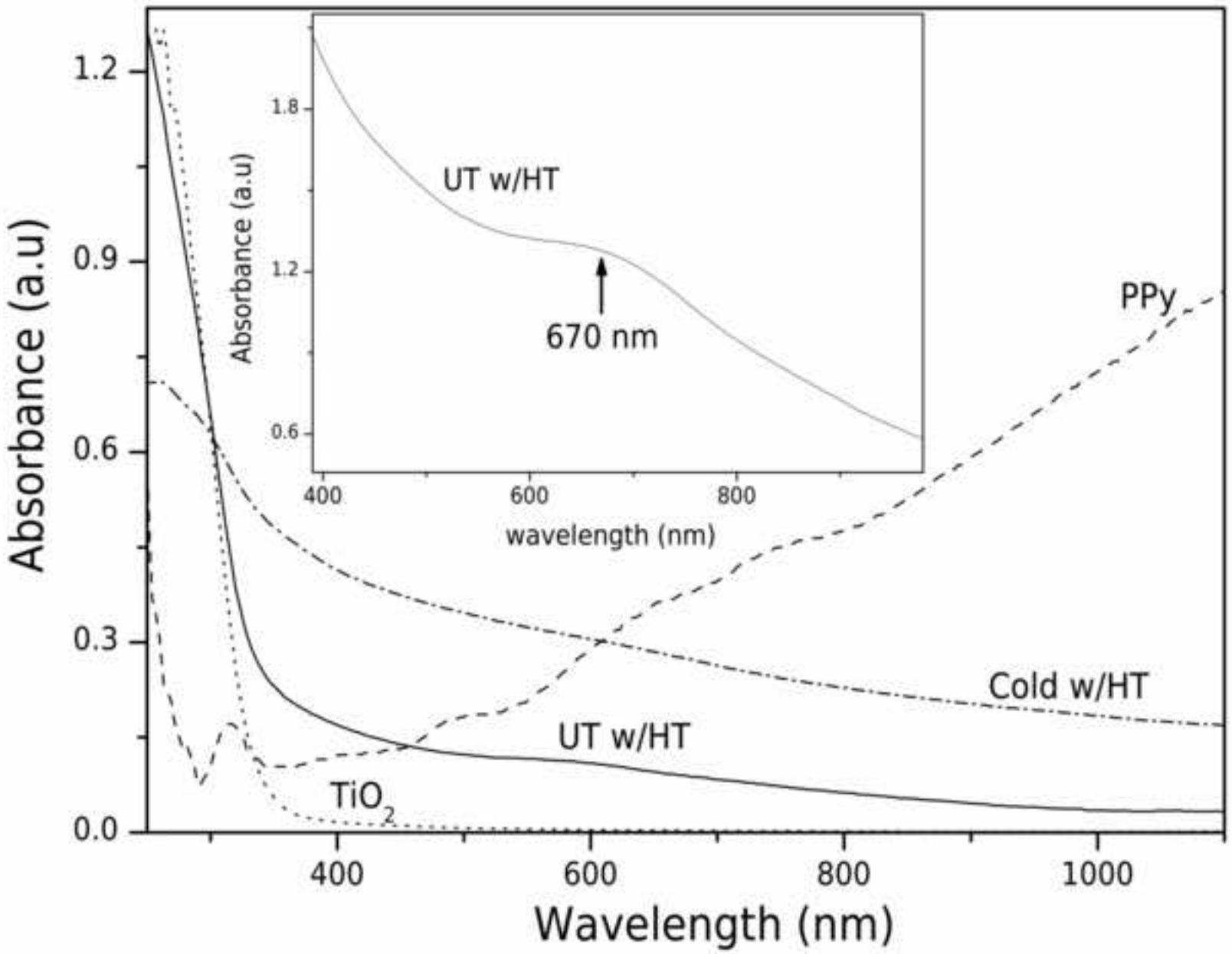

Figure 6b

ACCEPTED MANUSCRIPT

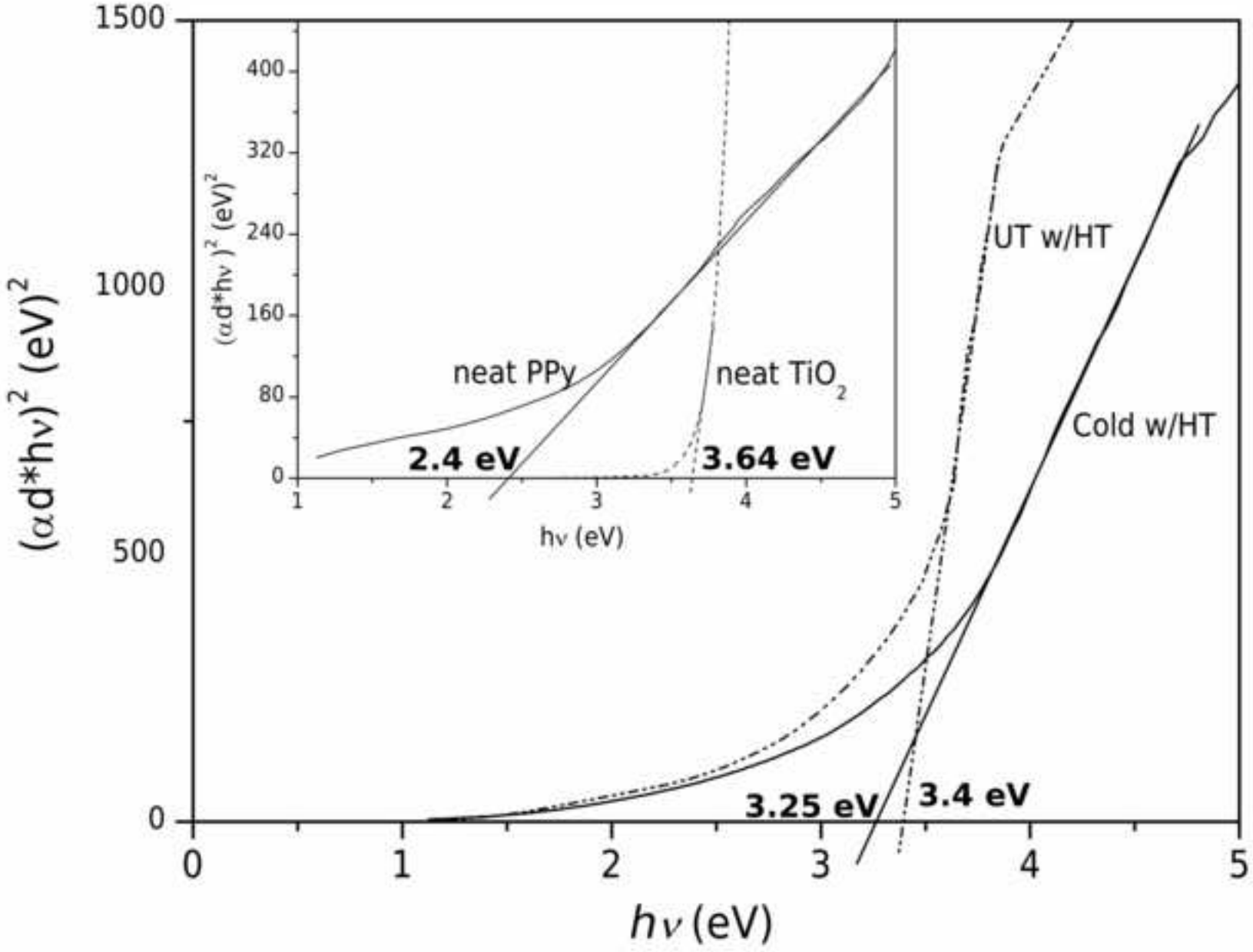

Figure 7

ACCEPTED MANUSCRIPT

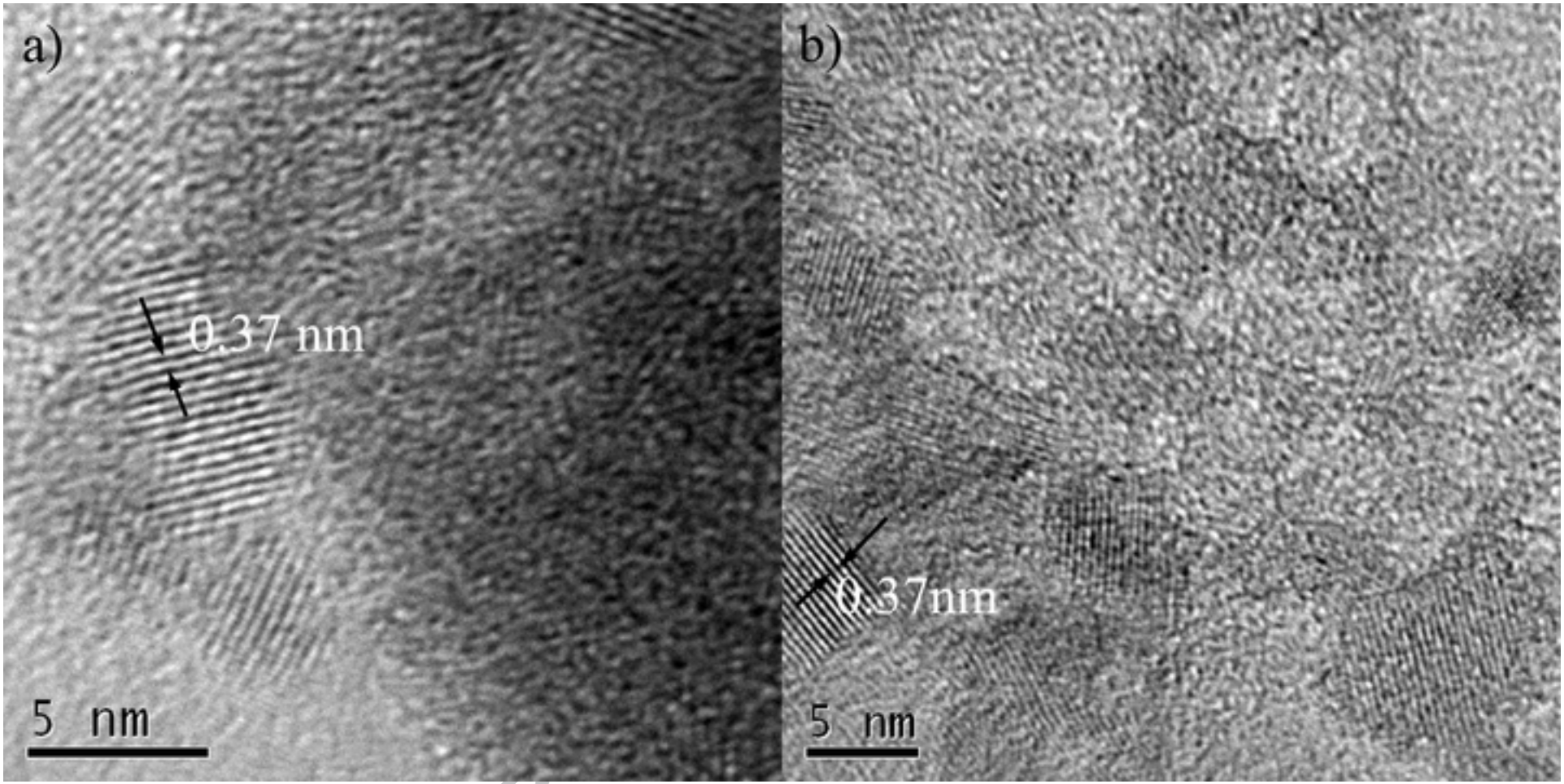

ACCEP

Figure 8

ACCEPTED MANUSCRIPT

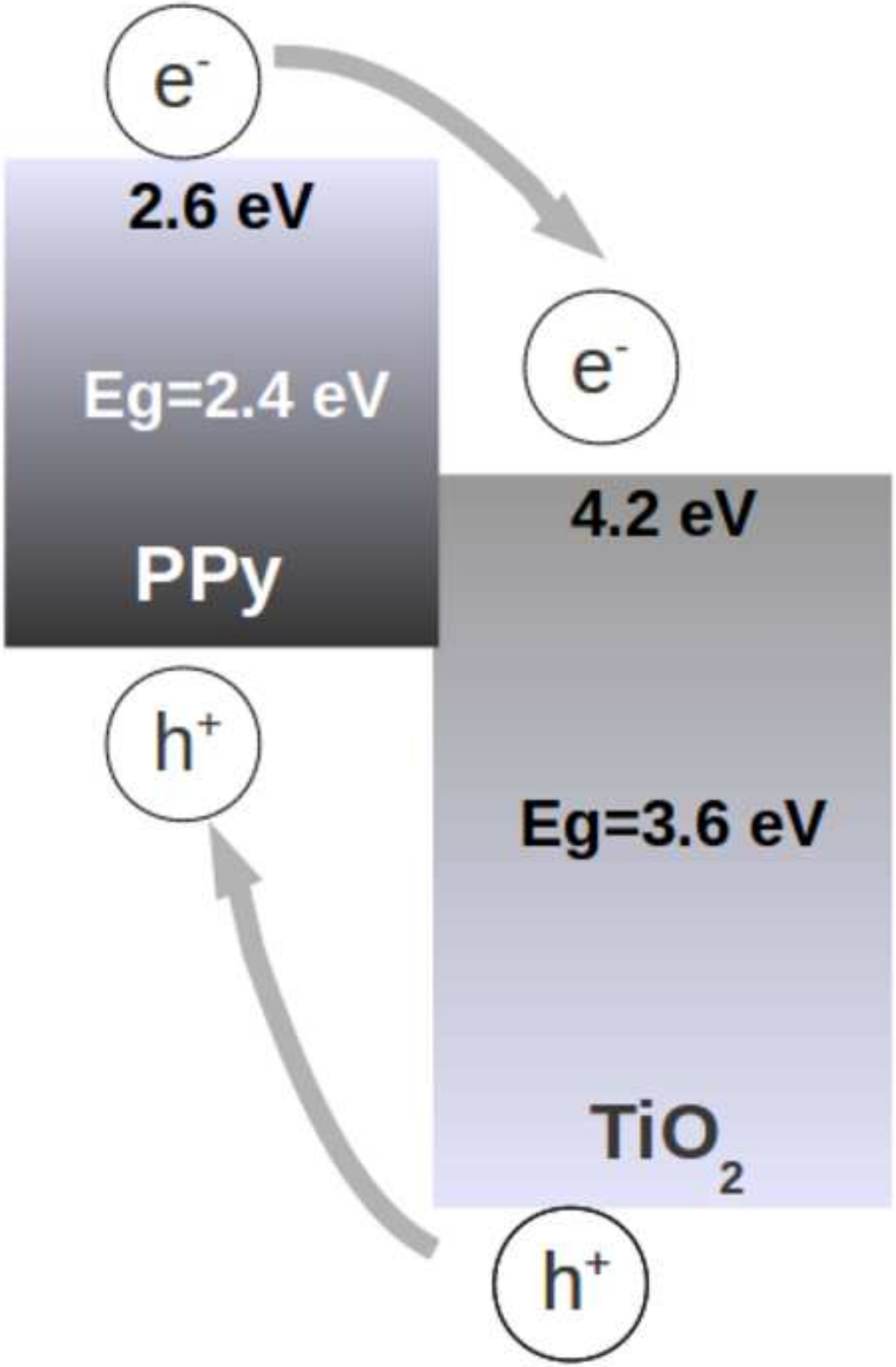

Figure 9

ACCEPTED MANUSCRIPT

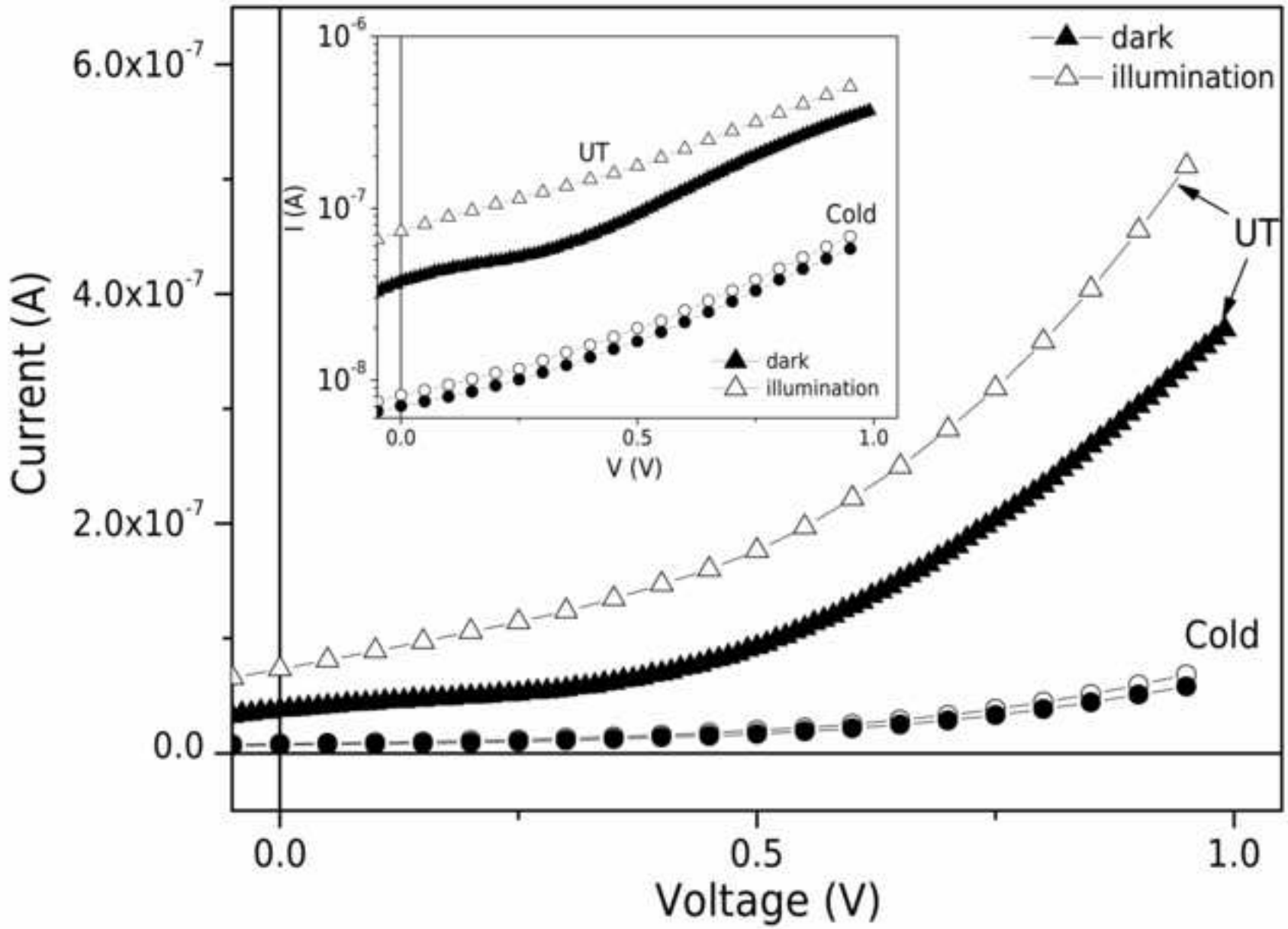

ACCEPTED MANUSCRIPT

Highlight

- Synthesis of hybrid nanocomposites by using a simple one-step under ultrasonication
- Direct obtention of crystalline titania in the nanocomposites by using low energy
- Nanocomposites with harvesting energy in the visible range for flexible solar cells

ACCEPTED MANUSCRIPT